Spider Silk Coatings as a Bioshield to Reduce Periprosthetic Fibrous Capsule Formation

ARTICLE *in* ADVANCED FUNCTIONAL MATERIALS · MAY 2014

Impact Factor: 11.81 · DOI: 10.1002/adfm.201302813

8 AUTHORS, INCLUDING:

Philip H Zeplin
LIPS Ludwigsburg Institute of Plastic Surgery
33 PUBLICATIONS **135** CITATIONS
SEE PROFILE

Gregor Lang
University of Bayreuth
6 PUBLICATIONS **54** CITATIONS
SEE PROFILE

ADVANCED FUNCTIONAL MATERIALS
www.afm-journal.de

www.MaterialsViews.com

Spider Silk Coatings as a Bioshield to Reduce Periprosthetic Fibrous Capsule Formation

*Philip H. Zeplin, Nathalie C. Maksimovikj, Martin C. Jordan, Joachim Nickel, Gregor Lang, Axel H. Leimer, Lin Römer, and Thomas Scheibel**

Medical grade silicones have been employed for decades in medical applications. The associated long-term complications, such as capsule formation and contraction have, however, not been fully addressed yet. The aim of this study is to elucidate if capsule formation and/or contraction can be mitigated by veiling the surface of the silicone during the critical phase after implantation. Medical grade silicone implants are homogeneously coated with a micrometer thin layer of recombinant spider silk proteins. Biocompatibility analysis in vitro and in vivo focuses on specific physiological reactions. Applying quantitative methods for the determination of marker-specific gene expression and protein concentration, it is detected that the silk coating inhibits fibroblast proliferation, collagen I synthesis, and differentiation of monocytes into CD68-positive histiocytes. It significantly reduces capsule thickness, post-operative inflammation, synthesis and re-modeling of extracellular matrix, and expression of contracture-mediating factors. Therefore, coatings made of recombinant spider silk proteins considerably reduce major post-operative complications associated with implantation of silicone-based alloprosthetics, such as capsular fibrosis and contraction, rendering spider silk coatings a bioshield for such implants.

1. Introduction

Medical grade silicones are silicones tested for biocompatibility and are appropriate to be used for medical applications. Importantly, long-term biocompatibility assessments of medical grade silicones for permanent implantation are available for breast implants (since 1963)[1] and intraocular lenses (since 1978)[2] only. An excessive formation of a fibrous capsule enclosing medical grade silicones of every kind is part of a patho-physiologic reaction, which can nowadays still not be sufficiently controlled and suppressed. In the reported cases, function may be lost and re-operation may be required. One of the largest fields of application of medical grade silicones is plastic and reconstructive breast surgery. Here, silicone implants are routinely used for the primary and secondary reconstruction of the female breast after mamma ablation or dysplasia and in cosmetic operations. The most prominent and specific complication is periprosthetic capsular fibrosis. It mostly occurs during the first year after surgery at incidence rates between 4.3–26.9%,[3,4] impairs the wellbeing of the affected patients by a severe feeling of tension and pressure, and may eventually result in considerable pain and tissue deformation. One year after implantation, the cumulative risks associated with capsule formation further increases.[5] The underlying mechanisms of capsule contracture development have been discussed controversially in literature.[6] Amongst the reasons for late capsule contracture, missing biocompatibility of the implanted material seems to play a prominent role, besides clinical factors such as infections, postoperative hematomas or seromes.[7]

Various strategies have been tested to improve the biocompatibility and to lower the risk of fibrosis of medical grade silicones by modifying their surfaces,[8] but none showed beneficial effects, a prerequisite to enter clinical trials. Here, we tested recombinant spider silk due to its general excellent biocompatibility and the mechanical resilience (**Figure 1**A).[10] A protein of the silk of the European garden spider *Araneus diadematus* has been previously used as a blueprint for the design of the recombinant spider silk protein eADF4(C16).[11] Recently, the protein has passed a series of preclinical safety tests including acute systemic toxicology and immunogenicity with no dose-limiting

Dr. P. H. Zeplin
Universitätsklinikum Leipzig
Department für Operative Medizin
Abteilung für Plastische
Ästhetische und spezielle Handchirurgie
Liebigstr. 20 04103, Leipzig, Germany
Dr. N. C. Maksimovikj, A. H. Leimer, Dr. L. Römer
AMSilk GmbH, Am Klopferspitz 19
82152, Planegg/Martinsried, Germany
Dr. M. C. Jordan
Universitätsklinikum Würzburg
Klinik für Unfall-, Hand-
Plastische und Wiederherstellungschirurgie
Oberdürrbacher Str. 2
97080, Würzburg, Germany
Dr. J. Nickel
Universitätsklinikum Würzburg
Lehrstuhl für Tissue Engineering und Regenerative Medizin (TERM)
Röntgenring 11, 97070, Würzburg, Germany
G. Lang, Prof. T. Scheibel
Lehrstuhl Biomaterialien
Universität Bayreuth
Universitätsstr. 30
Bayreuth, 95440, Germany
E-mail: thomas.scheibel@bm.uni-bayreuth.de

DOI: 10.1002/adfm.201302813

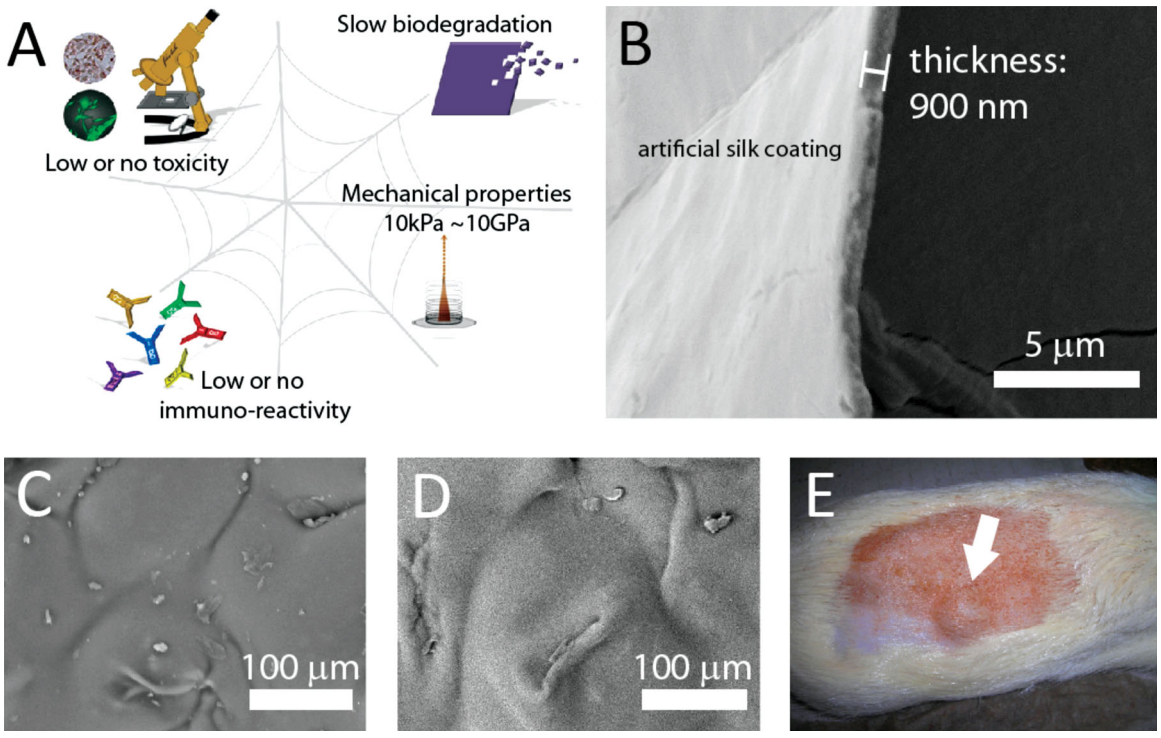

Figure 1. Coating of silicone implants with a recombinant spider silk protein. A) The recombinant spider silk protein eADF4(C16) shows no immunoreactivity and no toxicity. It can be processed into different morphologies with varying mechanical properties.[9] Silk structures in general are typically slowly biodegraded in vertebrate tissues.[21] B) Exemplary SEM image of a silk coating peeled of a silicone surface, revealing diameters from ≈1 to 6 µm depending on the dip coating procedure. C) SEM image of a non-coated silicone implant surface. D) SEM image of a eADF(C16) coated silicone implant surface. E) Photograph of a rat with a silk coated implant 3 months after implantation. Neither signs of inflammation nor symptoms of capsular fibrosis could be detected macroscopically.

toxicity or immune reactions observed (unpublished data). Since it has been shown that eADF4(C16) can be processed into various morphologies such as films, membranes and surface coatings,[12] here, medical grade silicone implants were coated with a micrometer thin eADF4(C16) layer (Figure 1B). Further, the influence of the silk coating on biocompatibility of the implant and capsular fibrosis was investigated.

2. Results and Discussion

2.1. Influence of a Spider Silk Coating on Biophysical and Biological Properties of a Silicone Surface

The water contact angle of uncoated textured silicone surfaces (Figure 1C) (control group, CG) was 139 ± 5°. After silk coating (Figure 1D) and sterilization (spider silk group, SG) the contact angle was significantly decreased to 101 ± 5°, indicating a less hydrophobic surface. At a coating thickness between ≈1 and 6 µm (Figure 1B), the microscopic roughness of the silicone surfaces was increased (silk group) showing a notable increase in microscopic surface area. However, the macroscopic roughness of uncoated and spider silk-coated silicones remained similar.

Proliferation of primary human fibroblasts on coated and uncoated silicone surfaces in cell culture experiments was significantly lower on spider silk-coated silicone compared to uncoated silicone and Permanox tissue culture plates serving as a negative control (**Figure 2**A–D). This observation is in agreement with Leal-Egana et al. 2012[13] where BALB/3T3 fibroblasts cultivated on eADF4(C16) film showed about 70% reduced adhesion and a strongly reduced cell proliferation when compared to standard culture dishes. Though ensuring increased hydrophilicity and superficial roughness, flat silk coatings (in contrast to fiber networks) show less protein adsorption than other surfaces (similar to anti-fouling surfaces) and, therefore, are not attractive for fibroblasts.

Although primary human monocytes showed an increased proliferation on spider silk-coated as well as uncoated silicone items in comparison to the negative control (Permanox) (Figure 2E–H), the differentiation into CD68-positive macrophages (histiocytes) was significantly decreased on spider silk-coated items in comparison to uncoated silicone ones.

2.2. Silk-Coated Silicone Implants are Well Tolerated in Sprague-Dawley Rats

Next, in vivo experiments were carried out in Sprague-Dawley rats to test the impact of the silk coatings on the performance of the silicone implant. All rats of two experimental groups with spider silk-coated and uncoated miniaturized silicone implants, implanted into subcutaneous pockets (Figure 1E),

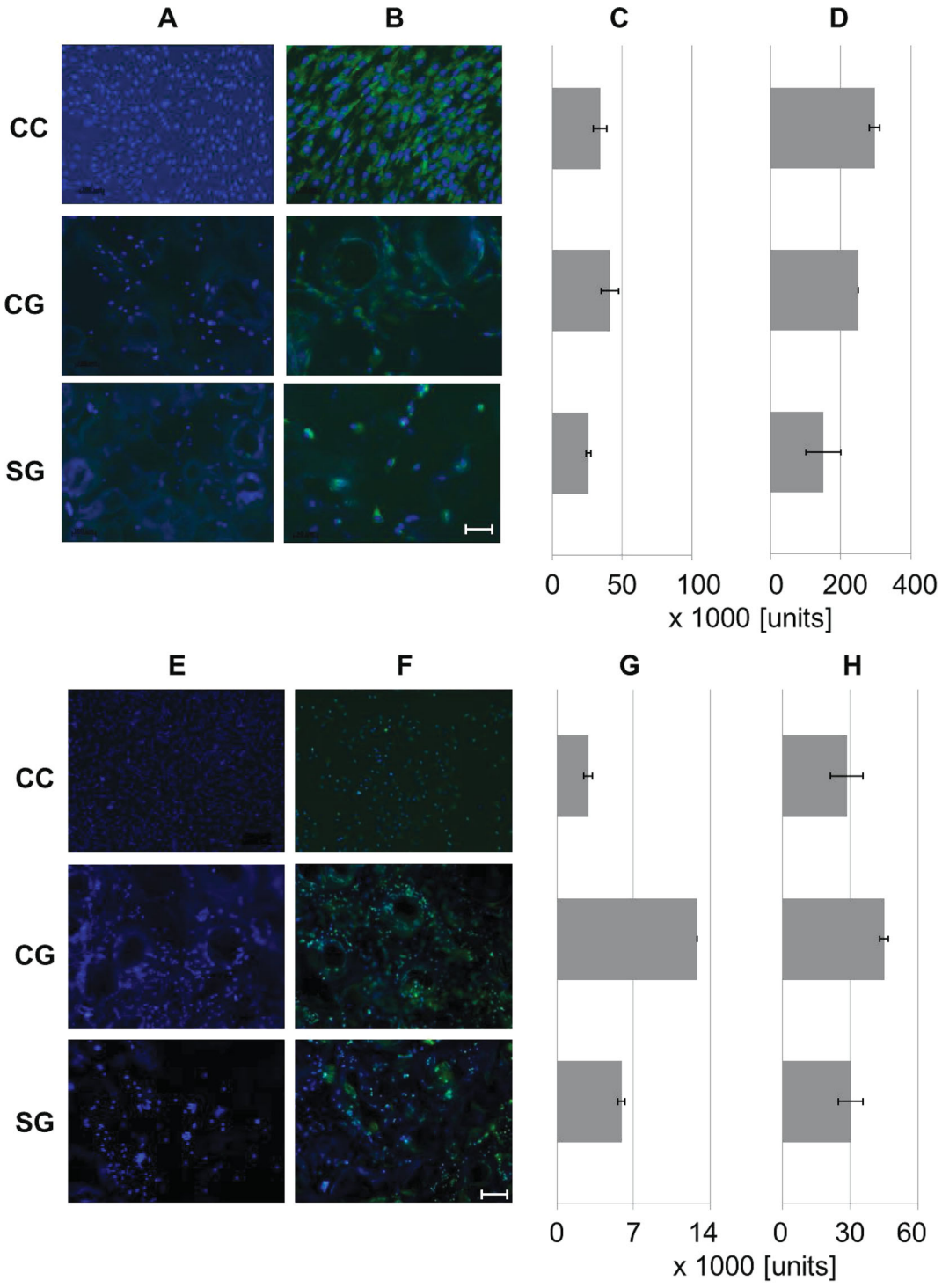

Figure 2. A) Fibroblast proliferation and collagen I biosynthesis were significantly reduced on spider silk surfaces in comparison to uncoated silicone and to Permanox, serving as a negative control. Primary fibroblasts were cultivated for 7 days and DAPI stained. B) same as (A) with additional immunostaining of collagen I (green) ((A) was treated with a secondary antibody as a control). C) Fluorescence intensity of PicoGreen (520 nm) representing total DNA content of the cultures corresponding to their total cell count. D) Luminescence intensity representing the total ATP content of the cultures corresponding to cell viability. E) Differentiation of primary monocytes into CD68-positive macrophages was inhibited on spider silk surfaces in comparison to uncoated silicone surfaces. Primary monocytes were cultivated for 7 days and DAPI stained. F) Treatment identical to (E) with additional immunostaining of CD68 ((E) was treated with a secondary antibody as a negative control). G) Fluorescence intensity of PicoGreen (520 nm) representing total DNA content of the cultures corresponding to the total cell count. H) Luminescence intensity representing the total ATP content of the cultures corresponding to cell viability. [CC] Negative control surface Permanox. [CG] Uncoated silicone surface. [SG] Spider silk-coated silicone surface. Scale bars (A–D) = 10 µm; scale bars (E–H) = 100 µm.

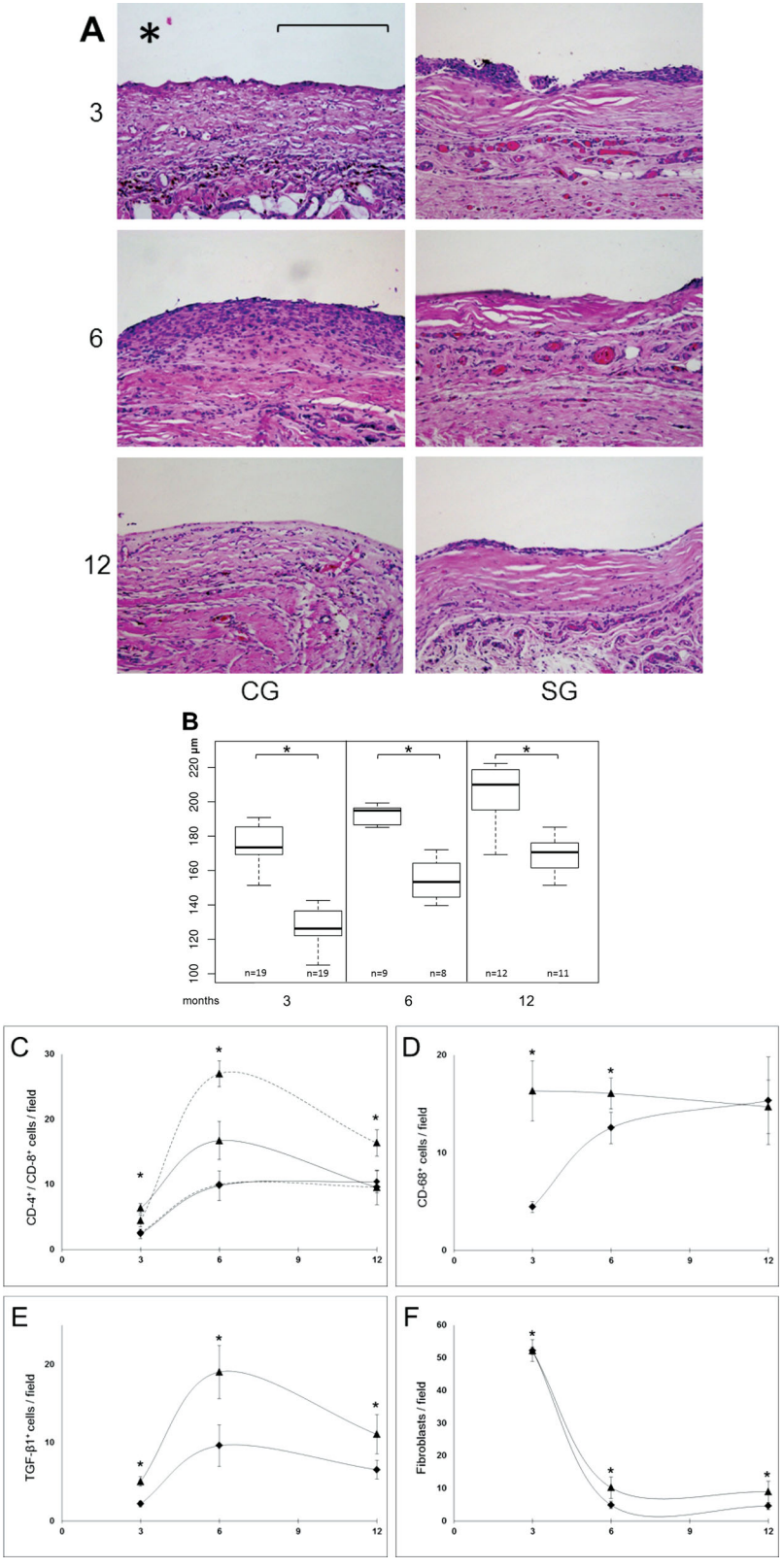

Figure 3. Spider silk coating of silicone implants results in reduced capsule thickness, altered collagen orientation and in reduced post-operative inflammation. A) Exemplary histological samples using hematoxylin and eosin staining of capsule biopsy specimens taken from the control (CG) and the silk group (SG) after 3, 6, and 12 months. Note the hypercytosis in CG and the differences in tissue morphology. Asterisk (*) marks the site of the silicone implant. Scale bar = 100 µm. B) Capsule thicknesses in µm expressed as median (interquartile range) after 3, 6, and 12 months in CG (left panel) and SG (right panel). $p \leq 0.05$ was considered significant (*). C) Number of $CD4^+$ (dashed line) and $CD8^+$ (solid line), D) $CD68^+$, E) TGF-beta1$^+$ cells, and F) fibroblasts in immunohistological sections of CG (▲) and SG (♦). Error bars indicate the mean standard deviation. Significance was determined using the Mann–Whitney U test. $p \leq 0.05$ was considered significant (*).

showed no signs of clinical abnormalities and survived until observation at three, six or twelve months, respectively. The spider silk coating was well tolerated with no observations of wound healing disorders, liver granulomes and alterations of lymph nodes that would have indicated infections or ectopic inflammation. After five as well as eleven months, one animal of the spider silk group had to be removed from the study since they had developed a cutaneous fibrous tumor spatially divided from the implant. The histopathological examination showed spindle cells arranged in a characteristic storiform pattern. The autopsy findings and the histopathological examination of the liver, spleen, lymph nodes and the periprosthetic capsule showed no histomorphological relationship to the implants or their coatings. Therefore, the tumors were classified as spontaneous neoplasms in aged Sprague-Dawley rats, as reported previously.[14]

2.3. Impact of Spider Silk Coating on Capsule Thickness and Collagen Orientation

The implants were removed from the animals three (two groups), six or twelve months post implantation together with the surrounding tissue capsules. Implant surfaces were examined for the remaining presence of eADF4(C16) spider silk protein by in-situ binding of specific antibodies followed by chemiluminescence imaging. Results indicated residual silk protein on the explants after implant periods up to 12 months (data not shown). Histological examination of the capsules enclosing uncoated silicone implants showed periprosthetic tissue rich in fibroblasts and histiocytes, mostly organized in multiple cell layers. This tissue showed collagen fibers in parallel and multidirectional orientations. In contrast, capsules surrounding spider silk-coated implants consisted of significantly fewer cells. These cells were organized in only two layers and contained fewer collagen fibers which were exclusively in parallel orientation (**Figure 3**A). This effect was accompanied by an altered capsule thickness within the silk group,

Table 1. qRT-PCR determination of inflammation, fibrosis, ECM synthesis, and contracture related markers.

Gene	3 months post implantation			12 months post implantation		
	fold change	*p* value	differently expressed	fold change	*p* value	differently expressed
Inflammation						
CD4	+1.51	0.497		+1.04	0.829	
CD8	–1.25	0.408		–1.01	0.926	
CD68	–1.19	0.813		–1.23	0.201	
IL6	–4.14	0.002	*	–2.00	0.975	
TNFα	–13.26	0.004	*	–2.63	0.126	
Fibrosis, cell proliferation						
Activin A	–1.94	0.035		–1.21	0.512	
CTGF	–7.72	<0.001	*	–1.64	0.294	
FAP-α	–14.52	0.002	*	+1.56	0.095	
Follistatin	–5.42	<0.001	*	–1.53	0.138	
PDGF	–1.68	0.011		–1.49	0.402	
TGFβ1	–14.62	<0.001	*	–2.90	0.007	*
TGFβ2	–9.18	<0.001	*	–0.71	0.159	
TGFβ3	–3.68	0.003	*	–1.07	0.734	
ECM synthesis and remodeling						
Col1	–4.56	0.031	*	–1.81	0.005	
Col3	–4.05	0.031	*	–1.46	0.168	
MMP2	–1.93	0.400		–1.60	0.054	
MMP9	–3.50	0.272		–0.39	0.844	
TIMP2	–4.43	0.003	*	–3.97	<0.001	*
Contracture (fibroblast-to-myofibroblast transdifferentiation)						
α-SMA	–2.63	0.408		–11.08	0.011	*
bFGF	–11.31	0.002	*	+1.10	1.000	
Vimentin	–5.31	0.031	*	–1.09	0.419	

*Genes were marked as differently expressed when the ratio of gene expression between spider silk coated and uncoated implants showed at least 2-fold up- (+) or down regulation (–), and the *p* value (Mann-Whitney U test) was ≤0.05.

which was reduced by 27.1 % (173 µm and 126 µm ($p = 0.002$)) after three, by 21.5 % (195 µm and 153 µm ($p = 0.003$)) after six, and by 18.5 % (210 µm and 171 µm ($p = 0.02$)) after twelve months (Figure 3B). Results obtained by qRT-PCR quantification of fibrosis-specific transcripts showed an impact of the silk coating on factors involved in fibrosis (**Table 1**): Expression levels of Follistatin, basic fibroblast growth factor (bFGF) and connective tissue growth factor (CTGF) were significantly altered in the silk group after three months indicating reduced fibrosis.

2.4. Impact of Spider Silk Coating on Post-Operative Inflammation

The early phase of inflammatory events as well as capsular fibrosis enveloping silicone implants is in general characterized by the appearance of CD4- and CD8-positive cells as well as increased expression of IL-6 and TNF-α.[15,16] Here, the extent of post-operative inflammatory events was first assessed by counting immunocytologically stained inflammation-specific cell types ($CD4^+$, $CD8^+$, $CD68^+$, $TGF\beta1^+$ and fibroblasts) in capsule tissue samples from spider silk-coated and uncoated silicone implants extracted three, six or twelve months after implantation. In all tissue samples a chronic inflammatory reaction was observed. $CD4^+$, $CD8^+$ and $TGF\text{-}\beta1^+$ cell numbers were highest after six months post-implantation followed by a decrease in specific cell abundance (Figure 3C,E). At the maximum, the cell numbers in the silk group were 1.6 to 3-fold lower than in the control group. Interestingly, $CD68^+$ cell abundance was reduced more than threefold in the silk group after three months followed by converging cell numbers after six and twelve months (Figure 3D). Fibroblast numbers of the control and the silk group differed only slightly but still significantly

(Figure 3F). Inflammation mediators were assayed along with IL-6 and TNF-α on their transcript level by quantitative RT-PCR (Table 1). Three months after implantation, the expression levels of IL-6 and TNF-α were reduced 4- and 13-fold, respectively, in periprosthetic tissues surrounding spider silk-coated implants. These differences were diminished twelve months after implantation. TGFβ1 was down-regulated more than 14-fold after three and 2.9-fold after twelve months. CD4, CD8, and CD68 levels showed no statistically significant differences.

Taken together, coating of the silicone implants with spider silk notably decreased the expression of all relevant measured factors. Especially, TNF-α expression which correlates with the degree of severity of foreign body-associated capsule formation,[17] was significantly lower even twelve months after implantation. CD68+ cells, also related with severity of fibrosis,[19] showed reduced proliferation on silk-coated silicone surfaces in vitro and in vivo. The critical steps during development of foreign body-associated fibrosis are triggered by the members of the TGFβ growth factor superfamily,[18] with TGFβ1 playing a dominant role in case of silicone.[19,20] We observed a strongly reduced expression of TGFβ1 and a reduced abundance of TGFβ1-positive cells in the presence of spider silk-coated implants when compared to uncoated equivalents. Accordingly, the level of CTGF which is implicated in various fibrotic disorders and induced in fibroblasts after activation with TGFβ mediating capsule formation[21] and fibrosis persistence[22] was significantly lower in the presence of silk coated silicone implants.

2.5. Impact of Spider Silk Coatings on Extracellular Matrix (ECM) Synthesis, Remodeling and Contracture-Mediating Factors

Wound remodeling within the first weeks after injury involves maturation and re-organization of the extracellular matrix (ECM), where collagen type III is mostly replaced by collagen type I. The expression levels of genes encoding early and late collagens (collagen III and I, respectively), matrix metalloproteinases MMP-2 and MMP-9, as well as tissue inhibitor of metalloproteinase-2 (TIMP-2) in periprosthetic tissues were assessed by qRT-PCR (Table 1). Expression levels of genes encoding collagen I, III and TIMP-2 differed significantly in the silk group in comparison to the control group after three months, indicating reduced ECM synthesis and remodeling. Concerning capsular fibrosis, the fraction of collagen type III of the total collagen was specified to be about 18%.[23] Reduced expression levels of collagen I and III were observed three months after implanting spider silk-coated silicone implants (Table 1). Interestingly, the relative down-regulation of the proteinase inhibitor TIMP-2 was still detectable twelve months after implantation, indicating a significant retardation and persisting attenuation of ECM remodeling.

Since myofibroblasts are also responsible for uncontrolled production of extracellular matrix proteins during the development of capsular fibrosis,[24] the extent of fibroblast trans-differentiation into myofibroblasts is a measure of fibrotic events. The genes of transforming growth factors β1, β2, and β3, responsible for triggering of cell proliferation, collagen synthesis and tissue contraction, were expressed at a considerably lower level in case of silk coated implants. Gene expression levels of bFGF and α-SMA clearly showed that the fibroblast-to-myofibroblast trans-differentiation was less pronounced in the vicinity of spider silk coated implants in comparison to uncoated implants. While bFGF induces the migration and proliferation of fibroblasts,[25] it also inhibits the formation of myofibroblasts by a) suppressing their trans-differentiation from fibroblasts[26] and b) enhancing the apoptosis of myofibroblasts—but not of fibroblasts.[27] Here, an 11-fold decrease of bFGF expression was observed in the periprosthetic tissue around silk-coated implants after three months, accompanied by a reduction of the fibroblast marker vimentin, a strongly reduced fibroblast number, and alpha smooth muscle actin (α-SMA) production (Table 1). In the silk group, vimentin expression was down-regulated more than 5-fold after three and α-SMA expression more than 11-fold after twelve months. Therefore, it can be concluded that coating of silicone implants with spider silk reduced fibroblast migration and proliferation. Associated with less fibroblasts the trans-differentiation into myofibroblasts was reduced and thus preserves the implant-embedding tissue from capsule formation and contraction.

Finally, we investigated the 170 kDa melanoma membrane-bound gelatinase fibroblast activation protein alpha (FAP-α) which is restricted to pathologic sites, including wounding, inflammation or fibrosis, but its gene is not expressed in most normal tissues. Even though it has no effect on the synthesis of the extracellular matrix, on the production of fibroblast growth factor (FGF) or on the expression of the gene of pro-inflammatory cytokine interleukin-6 (IL-6), it may increase the invasive capacity of fibroblasts, as observed in studies with keloid-derived fibroblasts.[28] Our results give rise to the assumption that FAP-α also plays an important role in the genesis of foreign body-associated fibrosis, and that coatings of spider silk effectively diminish this process. Further, the activin system seems to play a dominant role in keloid formation. Its involvement in fibrosis after implantation of alloplastic materials like silicone was not yet shown. Disequilibrium between activin A and follistatin, however, was previously shown to promote fibrotic diseases.[29] Here, the expression of both genes was decreased in the presence of the spider silk coating.

3. Conclusion

In summary, biocompatibility of medical grade silicones for long-term implantation is essentially determined by their surface, where the interaction with the body occurs. On one hand silicones are highly resistant against hydrolytic and enzymatic degradation, on the other hand they are considerably hydrophobic. Therefore, adhesion of unspecific proteins and cells is facilitated,[30] as well as attraction and proliferation of inflammatory and pro-fibrotic cells which trigger foreign body-associated fibrosis through the release of specific mediators.[31] Thereafter, a fibrotic capsule is formed, which is prone to undergo contracture as a severe deforming and painful complication. Based on these complications, attempts have previously been made to modify the surface of medical grade silicones with biomimetic compounds, such as phosphorylcholine[8] or

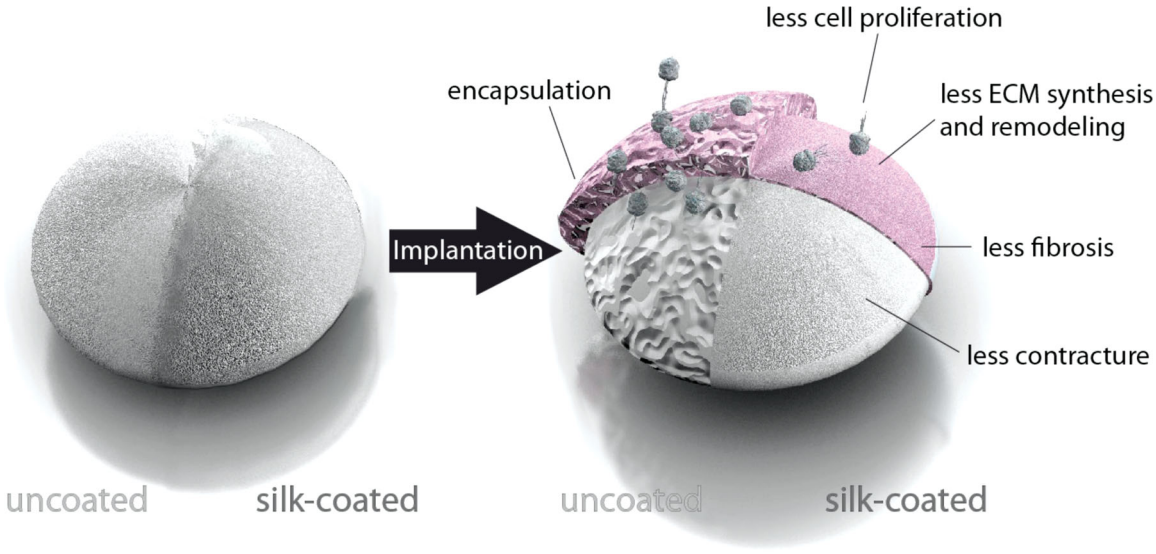

Figure 4. Model of the bioshield function of a spider silk coating on silicone implants.

collagen I,[32] but none showed a sufficient stability or a significantly improved biocompatibility. Here, coating of medical grade silicone implants using the recombinant spider silk protein eADF4(C16) resulted in a significant improvement of the implant's biocompatibility by effectively masking the implant's surface during the first months after implantation (**Figure 4**), which constitutes the immunologically most sensitive period. Since the recombinant spider silk protein is not subject to detectable immunological reactions, eADF4(C16) reflects an excellent candidate to resolve post-operative inflammatory and fibrotic complications and related discomfort often seen for silicone implants. Therefore, the developed spider silk coating provides the opportunity to significantly improve the medical performance of existing silicone implants with reasonable effort.

4. Experimental Section

If not stated differently, all reagents were purchased from Carl Roth and Sigma-Aldrich, Germany with p.a. quality.

Preparation of Silk Protein Solution: eADF4(C16) spider silk protein was produced as described earlier.[11] eADF4(C16) (AMSilk GmbH, Germany) was slowly dissolved at 1% w/v in 6 M guanidinium thiocyanate solution under gentle agitation. The identical volume of 50 mM Tris/HCl buffer pH 9 (Tris buffer) was slowly added, followed by dialysis against 50 mM Tris buffer at +4 °C overnight. Guanidinium thiocyanate remnants were removed by cross flow filtration at +4°C under constant addition of 50 mM Tris buffer. Subsequently, the protein was concentrated to 10.8 mg mL^{-1}.

Preparation of Silk-Coated Test Items: Textured silicone foils (diameter 2 cm, for in vitro study) and miniaturized silicone implants (diameter 2.6 cm, volume 3 mL, for in vivo study) were purchased from Polytech Health & Aesthetics, Dieburg, Germany. Prior to dip coating, the test items were rinsed in 70% ethanol and dried at room temperature. Then, the test items were dipped into the silk protein solution three times for 120 s followed by a drying interval of 300 s at room temperature. The silk coatings were fixed by dipping the coated samples in 1 M KH_2PO_4 solution for 120 s and air drying for 120 s. This procedure induces β-sheet formation rendering the silk coating water insoluble.[10–12] All test items were subsequently rinsed with 0.9% w/v NaCl. Miniaturized implants for in vivo experiments were sealed in sterile containers together with 500 µL fresh 0.9% NaCl solution. Textured silicone foils for in vitro experiments were placed in 24-well cell culture plates. The containers were sterilized by gamma-irradiation at 5 kGy.

Surface Characterization of Test Items: For analysis of wetability, static contact angles of water on coated and uncoated test items were determined using the ImageJ–LB-ADSA software (National Institute of Health, USA). For roughness analysis, coated and uncoated test items were submitted to 3D Laser Scanning Microscopy (LSM) analysis (VK-9700K, Keyence GmbH, Germany). For each type of test item, three LSM images at 1000-fold magnification were analyzed following DIN EN ISO standard 4287:1997 using the roughness tool of the VK-H1A1D/VK-H2A1E software (Keyence Deutschland GmbH, Frankfurt /Main, Germany). Quadratic roughness R_q was calculated from 20 independent lines per image. The arithmetic means of all parallel quadratic roughnesses R_q was expressed as Microscopic Line Roughness (MLRq).

Biocompatibility Test In Vitro: Fibroblasts were obtained from human foreskin from 5 circumcision patients. The tissue samples were fragmented, washed with phosphate-buffered saline, and then digested with Dispase (Invitrogen, Karlsruhe, Germany) for 16 h at +4 °C. After separating the epidermis from the dermis, the latter was treated with 0.2% collagenase (C-0130, Sigma-Aldrich, Hamburg, Germany) at 37 °C for 1 h to obtain fibroblast cells. After centrifugation and enzyme inhibition, dermal fibroblasts were cultured routinely in culture medium (Dulbecco's Modified Eagle Medium) and 10% fetal bovine serum (Invitrogen, Karlsruhe, Germany) at 37 °C, 5% CO_2.

To prepare monocytes, buffy coats were prepared from fresh human donor blood samples as published earlier.[33] Buffy coats were sedimented by re-centrifugation and labeled with CD14-specific magnetic microbeads (Miltenyi Biotec GmbH, Bergisch Gladbach, Germany) following the manufacturer's instructions. 10^7 cells were mixed with 80 µL buffer and 20 µL of microbead suspensions and incubated for 15 min at +4 °C. Subsequently, the cells were sedimented for 10 min at 30 *g* and +4 °C and resuspended in buffer at a total volume of 500 µL. CD14-specific cells were then separated magnetically, re-sedimented, counted and qualified by flow cytometry using CD14-specific FITC-labeled antibodies (Miltenyi Biotec GmbH, Bergisch Gladbach, Germany). The resulting monocyte precursor cells were seeded at a starting density

of 1×10^6 cells per mL and cultivated in RPMI-medium (Invitrogen, Karlsruhe, Germany).

In order to differentiate CD14-positive precursor cells into macrophages, the culture medium was first supplemented with 25 ng mL^{-1} M-CSF (macrophage colony-stimulating factor, Miltenyi Biotec GmbH, Bergisch Gladbach, Germany). After two days, the cells were resuspended, sedimented for 10 min at 500 *g* and room temperature, resuspended in the initial volume of growth medium and seeded again.

The cells were cultivated on test items and control surfaces. Fibroblasts were seeded at 1.2×10^4 and macrophages at 1×10^6 cells mL^{-1} as described above (four parallel cultures). Test items were spider silk-coated silicone, uncoated silicone and 8-well glass chamber slides equipped with Permanox surface, serving as a negative control.

Immunostaining and Detection: In vitro cell culture samples were incubated overnight with anti-collagen-I primary antibodies for fibroblast visualization (Acris Antibodies GmbH, Herford, Germany) and anti-CD68 primary antibodies for macrophage visualization (Abcam, Cambridge, UK). After washing with phosphate-buffered saline, samples were incubated with DAPI-Fluoromount G (Biozol Diagnostica, Eching, Germany) and visualized using a fluorescence microscope with filters set at 365nm (Zeiss Observer D1, Jena, Germany).

DNA Quantification and Cell Viability Determination: The total DNA of cultivated cells was quantified in triple determination using Quant-iTTM PicoGreen (Invitrogen, Darmstadt, Germany) following the manufacturer's instructions using a fluorometer (Thermo Fisher Scientific GmbH, Bremen, Germany).

Collective cell viability was determined by analyzing the total ATP content of the cultures using the CellTiter-Glo Luminescent Cell Viability Assay (Promega, Mannheim, Germany) following the manufacturer's instructions. The luminescent signal was determined luminometrically in triplicate at full bandwith (Infinite M200, Tecan Deutschland GmbH, Crailsheim, Germany).

Biocompatibility Test In Vivo: We aimed to mimick submammary prosthesis implantation in a subcutaneous pocket in adult rats. Permission (55.2-2531.01-19/09; Regierung von Unterfranken) was obtained from the animal ethics committee. Miniaturized textured silicone implants were implanted under the dorsal skin of 80 Sprague-Dawley rats (Harlan Winkelmann, Borchen, Germany). Each rat received one implant. The rats were divided in two groups: control group (CG), textured silicone implant ($n = 40$); spider silk group (SG), spider silk dip-coated textured silicone implant ($n = 40$).

The rats had free access to standard rat chow and water ad libitum and were housed five per cage, maintained at 21 ± 2 °C and a 12-hour light/ dark-cycle. General and wound check-up was performed regularly. Three (twice), six and twelve months after implantation, implantation sites of ten animals each were excised en bloc and processed for histologic (capsule thickness), immunocytochemical (specific cell type abundance) and molecular biology investigations (specific messenger RNA amount).

In order to prove test-retest reliability, the three months investigations were carried out twice at different time periods under identical conditions. Reliability was assessed using the Spearman correlation coefficient of determined capsule thicknesses and specific cell counts, where coefficients > 0.5 indicated large correlation.

Determination of Capsule Thickness: After withdrawal of implants and capsules under narcosis, the rats were sacrificed. Tissue samples were taken from all capsules. For histological examination, the samples were fixed in formalin (pH 7.4) and embedded in paraffin, cut into 4 µm slices and stained with hematoxylin and eosin (HE) or Masson Trichrome (MTC). Ten microscopic fields per capsule and staining technique were screened for their slimmest sites, thicknesses and morphology on the basis of the published capsule fibrosis classification score.[34] Correlation between assessed capsule thicknesses resulting from the two different staining techniques was calculated as described.

Specific Cell Counting: For the immunohistological examination, monoclonal antibodies against CD4, CD8, CD68/macrophage, TGF-beta1 and fibroblasts were acquired from MorphoSys AbD GmbH, Duesseldorf, Germany. The analysis was performed using a DP71 digital camera (Olympus Corp., Tokyo, Japan) integrated in a Canon BX51FT microscope (Canon, Inc., Tokyo, Japan) and the Cell∧F imaging system (Olympus Soft Imaging Solutions GmbH, Munich, Germany). The number of cells specifically labeled with antibodies against CD4, CD8, CD68, TGF-beta1, and fibroblasts was estimated by cell counting of ten microscopic fields per capsule.

Reference Gene Selection: For reference gene selection the Human Housekeeping Genes PCR Array was used for in vitro analysis and the Rat Housekeeping Genes PCR Array was used for in vivo analysis (Qiagen GmbH, Hilden, Germany). β-actin was found to be the most stably expressed reference gene and was used as internal control to normalize qRT-PCR.

Quantitative Determination of mRNA (qRT-PCR): Biopsies taken from each periprosthetic tissue were collected in RNAlater reagent (Qiagen, Hilden, Germany). Total RNA was isolated using Trizol reagent (Invitrogen, Darmstadt, Germany) according to the manufacturer's instructions. 1 µg of total RNA was used for cDNA synthesis using the ThermoScript real-time polymerase chain reaction (RT-PCR) System (Invitrogen, Darmstadt, Germany) according to the manufacturer's instructions. PCR was performed using GoTaq Flexi DNA polymerase (Promega, Madison, Wisconsin). Primers (Qiagen, Hilden, Germany) were mRNA-specific in order to avoid mal-amplification of DNA. An Opticon2 cycler (Biorad, Munich, Germany) was set to standard PCR conditions and an annealing temperature of 55 °C. The PCR products were stained with SybrGreen-Premix (Eurogentec, Seraing, Belgium). The system was calibrated by titration of the mRNA encoding β-actin. Results were expressed as the threshold cycle (Ct) of the specific target mRNA and as normalized threshold cycle (ΔCt) of the specific mRNA compared to that of the housekeeping gene β-actin. The fold change ratio for each gene ($2^{-\Delta\Delta Ct}$)[35] was compared between the spider silk treated (SG) and the untreated control group (CG) and was considered relevant when it was ≥ 2. Genes were reported as differently expressed between groups when the fold change ratio was at least 2-fold up- or down regulated, and the p value (Mann-Whitney U test[36]) was ≤ 0.05.

Statistical Analysis: Data analysis was performed using SPSS 15.0 (IBM Corp., USA). Results were calculated as means ± standard deviation (SD) or medians with interquartile range. For comparison among different groups the Mann-Whitney-U-Test[36] was used with significance assigned at $p \leq 0.05$ (*).

Acknowledgements

This work was generously supported by grant A-106-N of the Interdisciplinary Center of Clinical Research (IZKF), a component of the Würzburg University Hospital and SFB 840 TPA8 (TS).

The authors would like to thank Prof. Dr. H. Walles (Würzburg University Hospital, Chair of Regenerative Medicine and Tissue Engineering/ TERM), Prof. Dr. R. H. Meffert (Würzburg University Hospital, Department of Trauma, Hand, Plastic and Reconstructive Surgery), Prof. Dr. S. Langer, (Leipzig University Hospital and Medical School, Department of Operative Medicine, Division of Plastic, Aesthetic and Hand Surgery) for providing a good environment and facilities to complete this project and helpful discussions and Dr. M. Lehnerer, AMSilk GmbH, Martinsried for editing this publication. Further acknowledged are P. van Gelder (Würzburg University Hospital, Department of Trauma, Hand, Plastic and Reconstructive Surgery) for assistance in animal experiments, tissue preparation and analysis, A.K. Berninger (Würzburg University Hospital, Chair of Regenerative Medicine and Tissue Engineering/ TERM) for in-vitro cell cultivation and analysis, A. Schmidt (Universität Bayreuth, Biomaterialien) for providing SEM images and T. Huppmann (Universität Bayreuth, Biomaterialien) for experimental help.

Received: August 9, 2013
Revised: October 21, 2013
Published online: January 13, 2014

[1] G. P. Maxwell, A. Gabriel, *Clin. Plast. Surg.* **2009**, *36*, 1–13.
[2] G. U. Auffarth, D. J. Apple, *Ophthalmologe* **2001**, *98*, 1017–1028.
[3] A. Dancey, A. Nassimizadeh, P. Levick, *J. Plast. Reconstr. Aesthet. Surg.* **2012**, *65*, 213-218.
[4] T. F. Henriksen, J. P. Fryzek, L. R. Hölmich, S. Friis, J. K. McLaughlin, A. P. Høyer, K. Kjøller, J. H. Olsen. *Ann. Plast. Surg.* **2005**, *54*, 343–351.
[5] M. Marques, S. A. Brown, I. Oliveira, M. N. Cordeiro, A. Morales-Helguera, A. Rodrigues, J. Amarante, *Plast. Reconstr. Surg.* **2010**, *126*, 769–778.
[6] M. Embrey, E. E. Adams, B. Cunningham, W. Peters, V. L. Young, G. L. Carlo, *Aesthetic Plast. Surg.* **1999**, *23*, 197–206.
[7] S. Schreml, N. Heine, M. Eisenmann-Klein, L. Prantl, *Ann. Plast. Surg.* **2007**, *59*, 126–130.
[8] P. H. Zeplin, A. Larena-Avellaneda, M. Jordan, M. Laske, K. Schmidt, *Ann. Plast. Surg.* **2010**, *65*, 560–564.
[9] J. G. Hardy, L. M. Roemer, T. Scheibel, *Polymer* **2008**, *49*, 4309–327.
[10] K. Spiess, A. Lammel, T. Scheibel, *Macromol. Biosci.* **2010**, *10*, 998–1007.
[11] D. Huemmerich, C. W. Helsen, J. Oschmann, R. Rudolph, T. Scheibel, *Biochemistry* **2004**, *43*, 13604–1312.
[12] A. Leal-Egaña, T. Scheibel, *J. Mater. Chem.* **2012**, *22*, 14330–14336.
[13] A. Leal-Egaña, G. Lang, C. Mauerer, J. Wickinghoff, M. Weber, S. Geimer, T. Scheibel, *Advanced Biomaterials* **2012**, *14*, B67–B75.
[14] M. Chandra, M. G. Riley, D. E. Johnson, *Arch. Toxicol.* **1992**, *66*, 496–502.
[15] A. F. Wells, S. Daniels, S. Gunasekaran, K. W. Wells, *Ann. Plast. Surg.* **1994**, *33*, 1-5.
[16] D. Granchi, D. Cavedagna, G. Ciapetti, S. Stea, P. Schiavon, R. Giuliani, A. Pizzoferrato, *J. Biomed. Mater. Res.* **1995**, *29*, 197–202.
[17] K. T. Tan, D. Wijeratne, B. Shih, A. D. Baildam, A. Bayat, *Eur. Surg. Res.* **2010**, *45*, 327–332.
[18] Y. Abe, T. Minegishi, P. C. Leung, *Growth Factors* **2004**, *22*, 105–110.
[19] M. Kamel, K. Protzner, V. Fornasier, W. Peters, D. Smith, D. Ibanez, *J. Biomed. Mater. Res.* **2001**, *58*, 88–96.
[20] A. Kuhn, S. Singh, P. D. Smith, F. Ko, R. Falcone, W. G. Lyle, S. P. Maggi, K. E. Wells, M. C. Robson, *Ann. Plast. Surg.* **2000**, *44*, 387–391.
[21] M. K. Mazaheri, G. S. Schultz, T. D. Blalock, H. H. Caffee, G. A. Chin, *Ann. Plast. Surg.* **2000**, *50*, 263–268.
[22] S. Chujo, F. Shirasaki, S. Kawara, Y. Inagaki, T. Kinbara, M. Inaoki, M. Takigawa, K. Takehara, *J. Cell Physiol.* **2005**, *203*, 447–456.
[23] L. P. Bucky, H. P. Ehrlich, S. Sohoni, J. W. May, *Plast. Reconstr. Surg.* **1994**, *93*, 1123–1131.
[24] S. Piera-Velazquez, Z. Li, S. A. Jimenez, *Am. J. Pathol.* **2011**, *179*, 1074–1080.
[25] T. Makino, M. Jinnin, F. C. Muchemwa, S. Fukushima, H. Kogushi-Nishi, C. Moriya, T. Igata, A. Fujisawa, T. Johno, H. Ihn, *Br. J. Dermatol.* **2010**, *162*, 717–723.
[26] G. E. Spyrou, I. L. Naylor, *Br. J. Plast. Surg.* **2002**, *55*, 275–282.
[27] M. Abe, Y. Yokoyama, O. Ishikawa, *Eur. J. Dermatol.* **2012**, *22*, 46–53.
[28] K. Dienus, A. Bayat, B. F. Gilmore, O. Seifert, *Arch. Dermatol. Res.* **2010**, *302*, 725–731.
[29] A. Mukhopadhyay, S. Y. Chan, I. J. Lim, D. J. Phillips, T. T. Phan, *Am. J. Physiol. Cell. Physiol.* **2007**, *292*, C1331–1338.
[30] A. Pajkos, A. K. Deva, K. Vickery, C. Cope, L. Chang, Y. E. Cossart, *Plast. Reconstr. Surg.* **2003**, *111*, 1605–1611.
[31] A. Hezi-Yamit, C. Sullivan, J. Wong, L. David, M. Chen, P. Cheng, D. Shumaker, J. N. Wilcox, K. Udipi, *J. Biomed. Mater. Res. A.* **2009**, *90*, 133–141.
[32] J. Hauser, J. Zietlow, M. Köller, S. A. Esenwein, H. Halfmann, P. Awakowicz, H. U. Steinau, *J. Mater. Sci. Mater. Med.* **2009**, *20*, 2541–2548.
[33] L. A. Kay, D. E. Lock, *J. Clin. Pathol.* **1985**, *38*, 1405–1408.
[34] P. Wilflingseder, A. Probst, G. Mikuz, *Chir. Plastic.* **1974**, *2*, 215.
[35] K. J. Livak, T. D. Schmittgen, *Methods* **2001**, *25*, 402–408.
[36] H. B. Mann, D. R. Whitney, *Ann. Math. Stat.* **1947**, *18*, 50–60.